Thermal Dissociation of the TIK$(H^+)_2$ Tripeptide. Mechanisms, Kinetic Parameters, and Comparison with CID

Zahra Homayoon,[a] Subha Pratihar,[a] Edward Dratz,[b] Ross Snider,[c]
Riccardo Spezia,[d] George L. Barnes,[e] Veronica Macaluso,[d]
Ana Martin Somer,[d] and William L. Hase[a]*

[a]Department of Chemistry and Biochemistry
Texas Tech University
Lubbock, Texas 79409-1061 USA

[b]Department of Chemistry and Biochemistry
Montana State University
Bozeman, Montana 59717 USA

[c]Department of Electrical and Computer Engineering
Montana State University
Bozeman, Montana 59717 USA

[d]Laboratoire Analyse et Modélisation pour la Biologie et l'Environnement
Université d'Evry Val d'Essonne
UMR 8587 CNRS-CEA-UEVE
Bd. F. Mitterrand, 91025 Evry Cedex, France

[e]Department of Chemistry and Biochemistry
Siena College
Loudonville, NY 12211, USA

Figure S1. Optimized geometry of a conformer of $TIK(H^+)_2$ determined by RM1. The relative energy to the global minimum is given in kJ/mol.

Figure S2. Mechanisms for dissociation pathways 9-20.

Figure S3. *m/z* product distribution as obtained from RM1 trajectories at 1250 K halted at 90 ps.

Figure S4. *m/z* product distribution as obtained from RM1 trajectories at 1500 K halted at 30 ps.

Figure S5. *m/z* product distribution as obtained from RM1 trajectories at 2000 K halted at 10 ps.

Figure S6. *m/z* product distribution as obtained from RM1 trajectories at 2500 K halted at 1.5 ps.

Figure S7. The plot of $N(t)/N(0)$ versus t for high energy conformer trajectories using RM1.

Figure S8. The plot of $N(t)/N(0)$ versus t for 100 AM1 trajectories.

Figure S9. The secondary dissociations observed for the primary dissociation pathways 1, 3, 4, 6, 7, 8, 9, 13, 15, 17, and 18 from the AM1 trajectories. The number of trajectories which followed each pathway is identified in parentheses.

Figure S10. *m/z* product distribution as obtained from AM1 trajectories halted at 30 ps.

Figure S11. *m/z* product distribution as obtained from RM1 trajectories for CID at E_{rel} = 1255 kJ/mol.

Figure S12. Energy transfer distribution as obtained by collisional simulations of $TIK(H^+)_2$ with N_2 for a collision energy of 1255 kJ/mol.

Table S1. Probabilities of $TIK(H^+)_2$ Dissociation Pathways versus Temperature from RM1 Direct Dynamics Simulations for pathways 1-20.

Table S2. Probabilities of different fragment ions (*m/z*) from RM1 calculations at 1250 K.

Table S3. Probabilities of different fragment ions (*m/z*) from RM1 calculations at 1500 K.

Table S4. Probabilities of different fragment ions (*m/z*) from RM1 calculations at 2000 K.

Table S5. Probabilities of different fragment ions (*m/z*) from RM1 calculations at 2500 K.

Table S6. Abundances of different fragment ions (*m/z*) from AM1 calculations when the trajectories were halted at 30 ps (2000K).

Table S7. Probabilities of different fragment ions (*m/z*) from RM1 calculations for CID at 1255 kJ/mol.

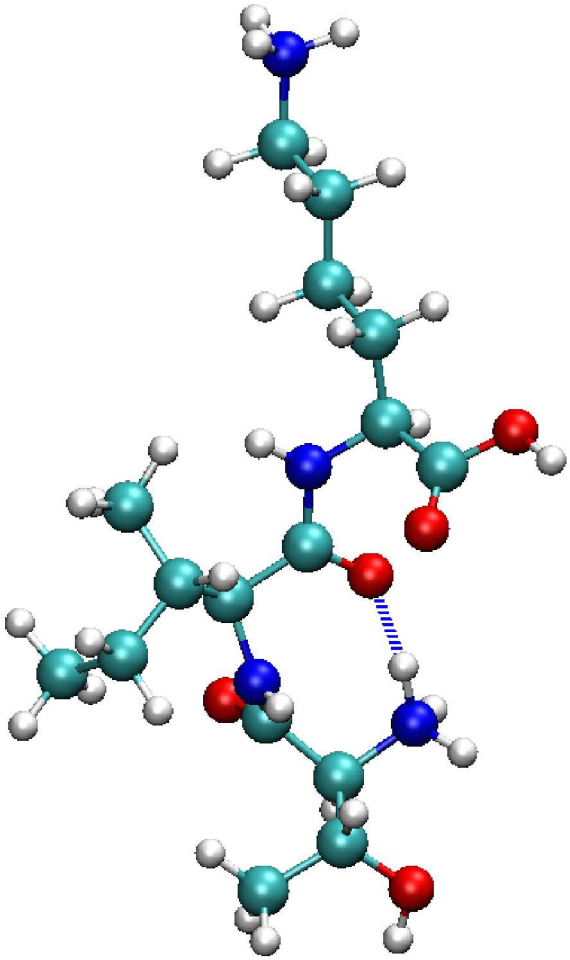

38.4

Figure S1.

Pathway 9

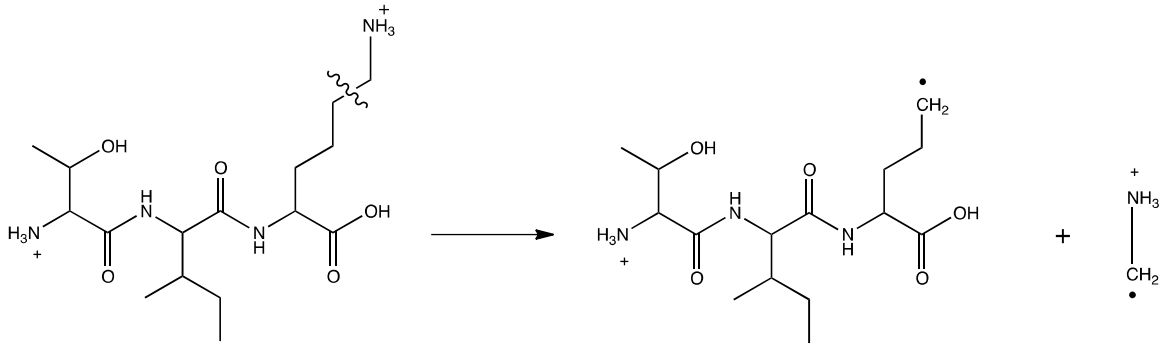

m/z 331 *m/z* 31

Pathway 10

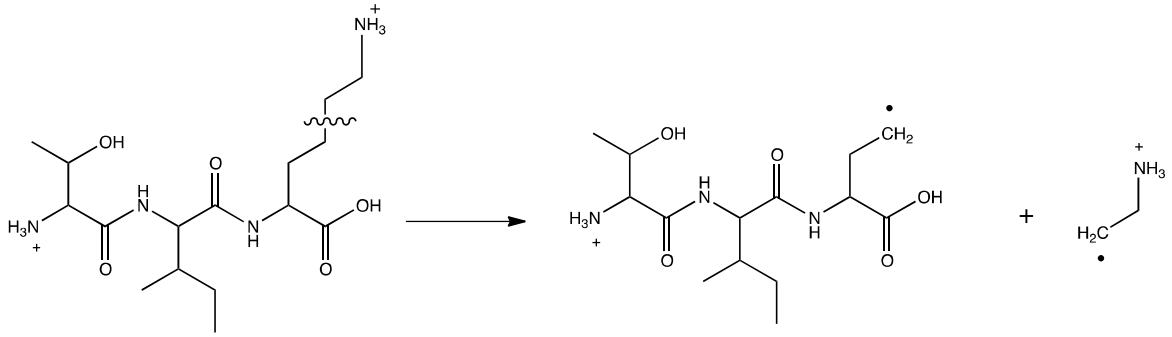

m/z 317 *m/z* 45

Pathway 11

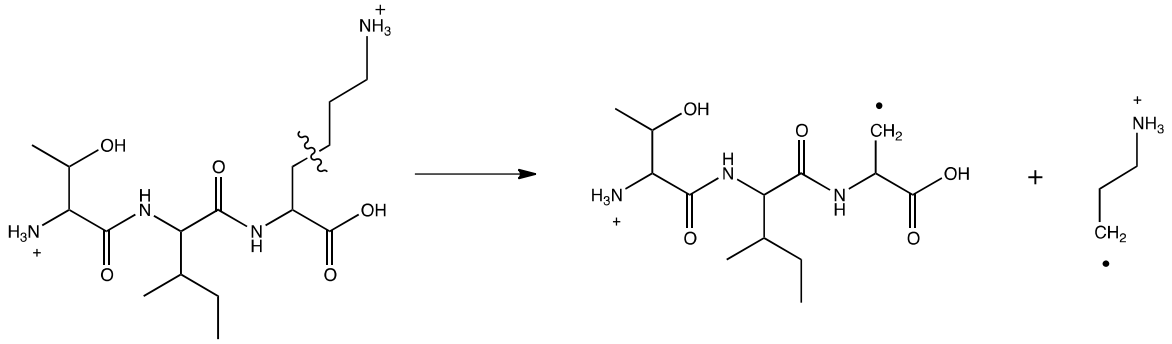

m/z 303 *m/z* 59

Pathway 12

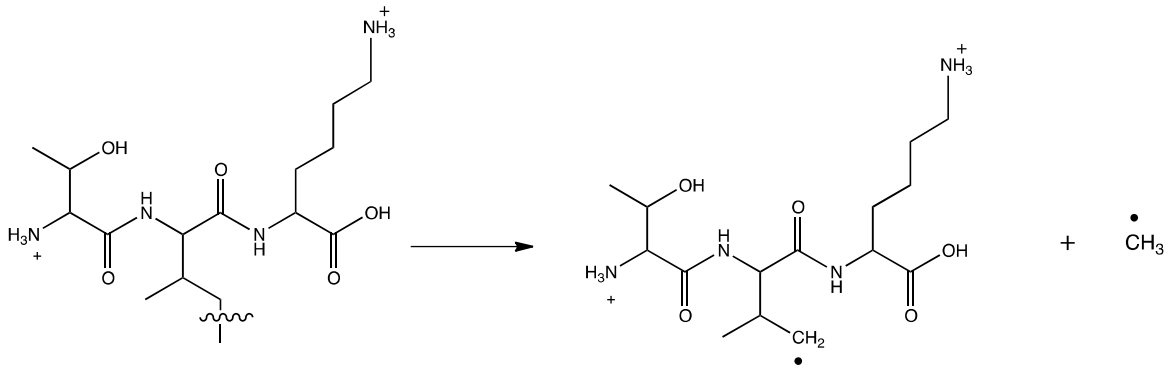

m/z 173.5

Pathway 13

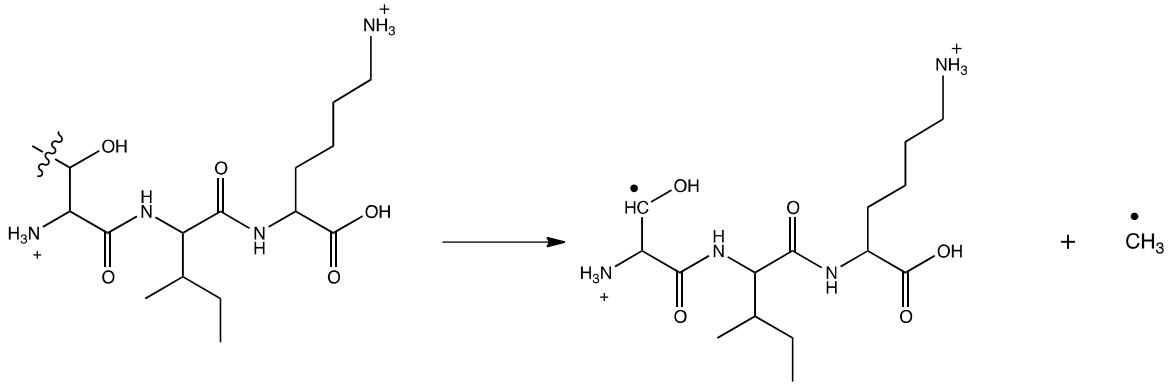

m/z 173.5

Pathway 14

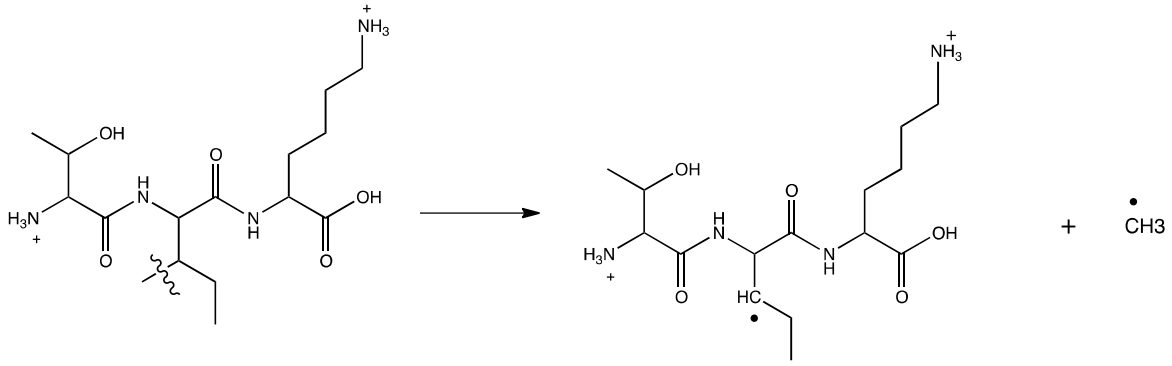

m/z 173.5

Pathway 15

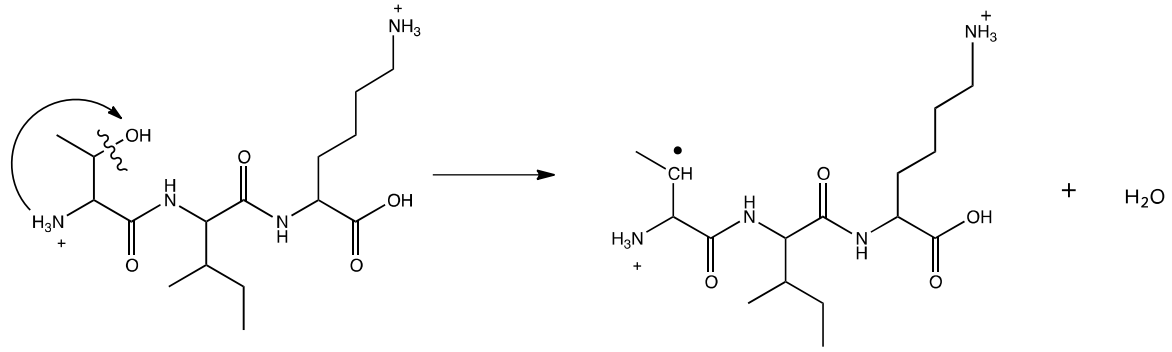

m/z 172

Pathway 16

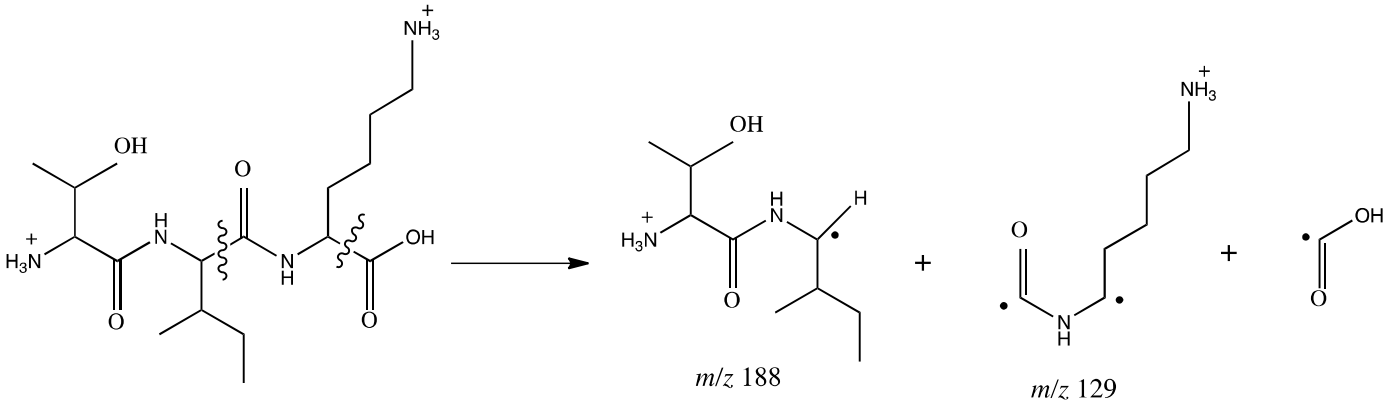

m/z 188

m/z 129

Pathway 17

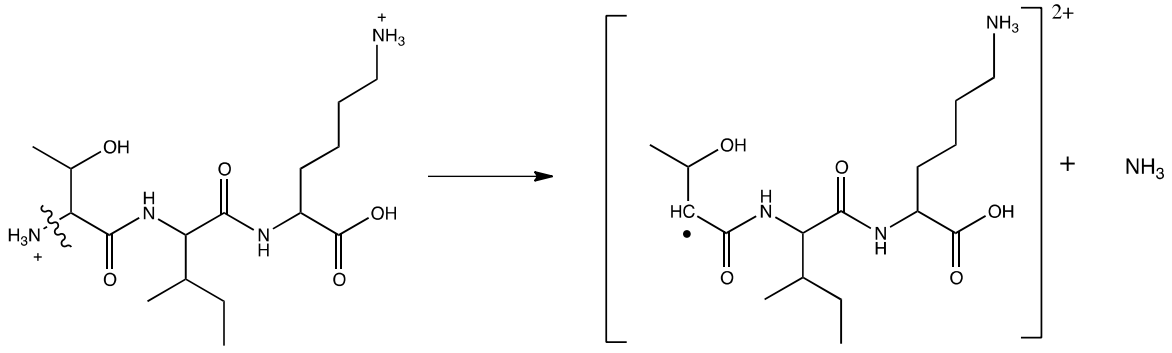

m/z 172.5

Pathway 18

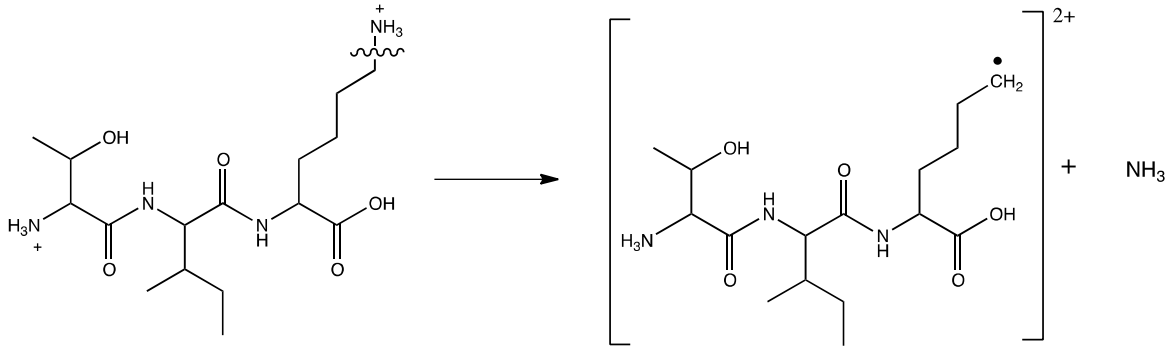

m/z 172.5

Pathway 19

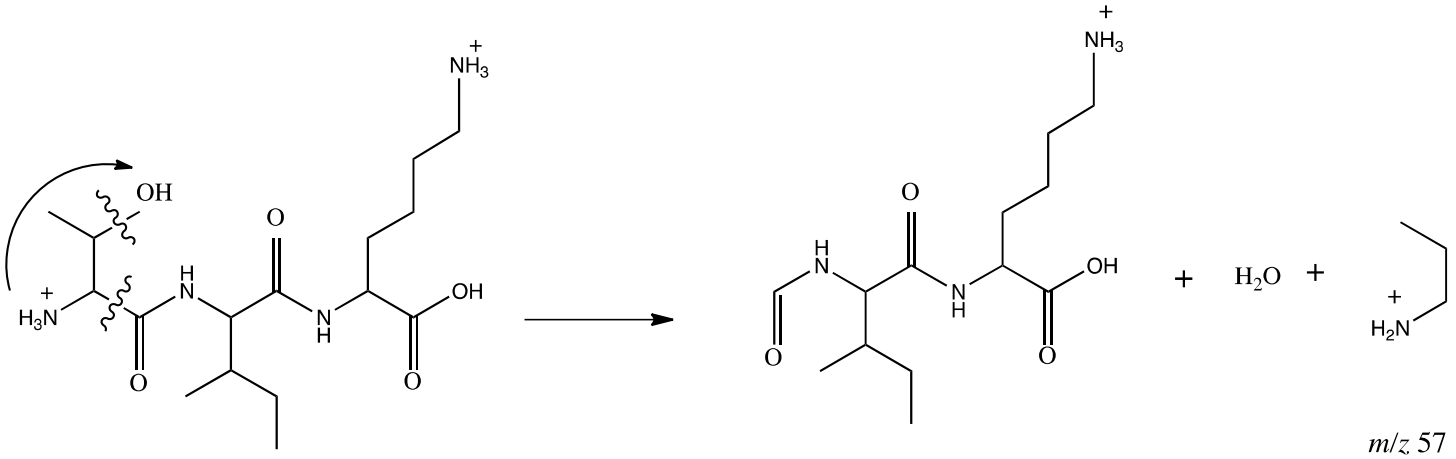

m/z 287

m/z 57

Pathway 20

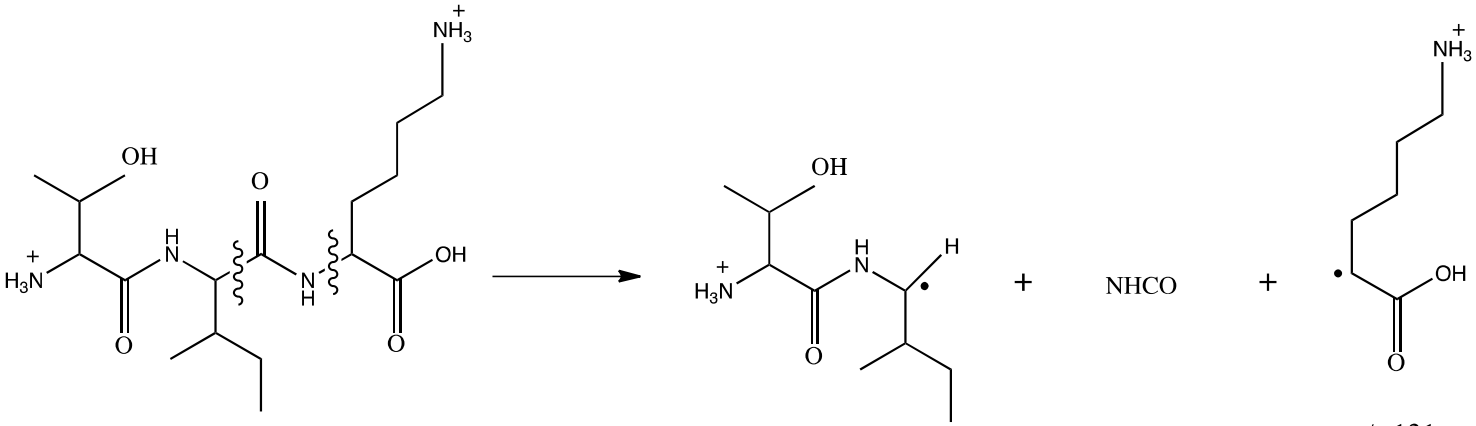

m/z 188

m/z 131

Figure S2.

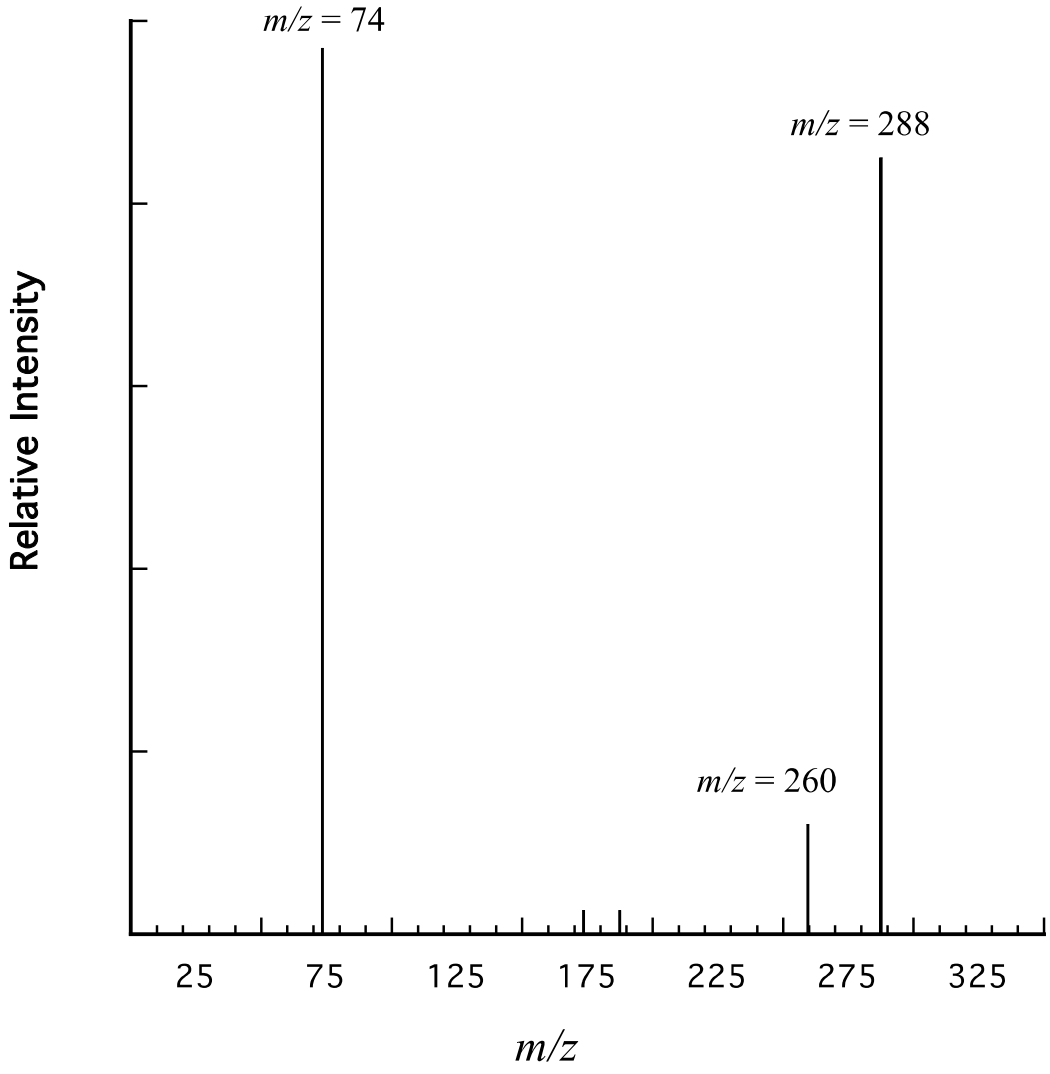
m/z = 74
m/z = 288
m/z = 260
Relative Intensity
25
75
125
175
225
275
325
m/z

Figure S3.

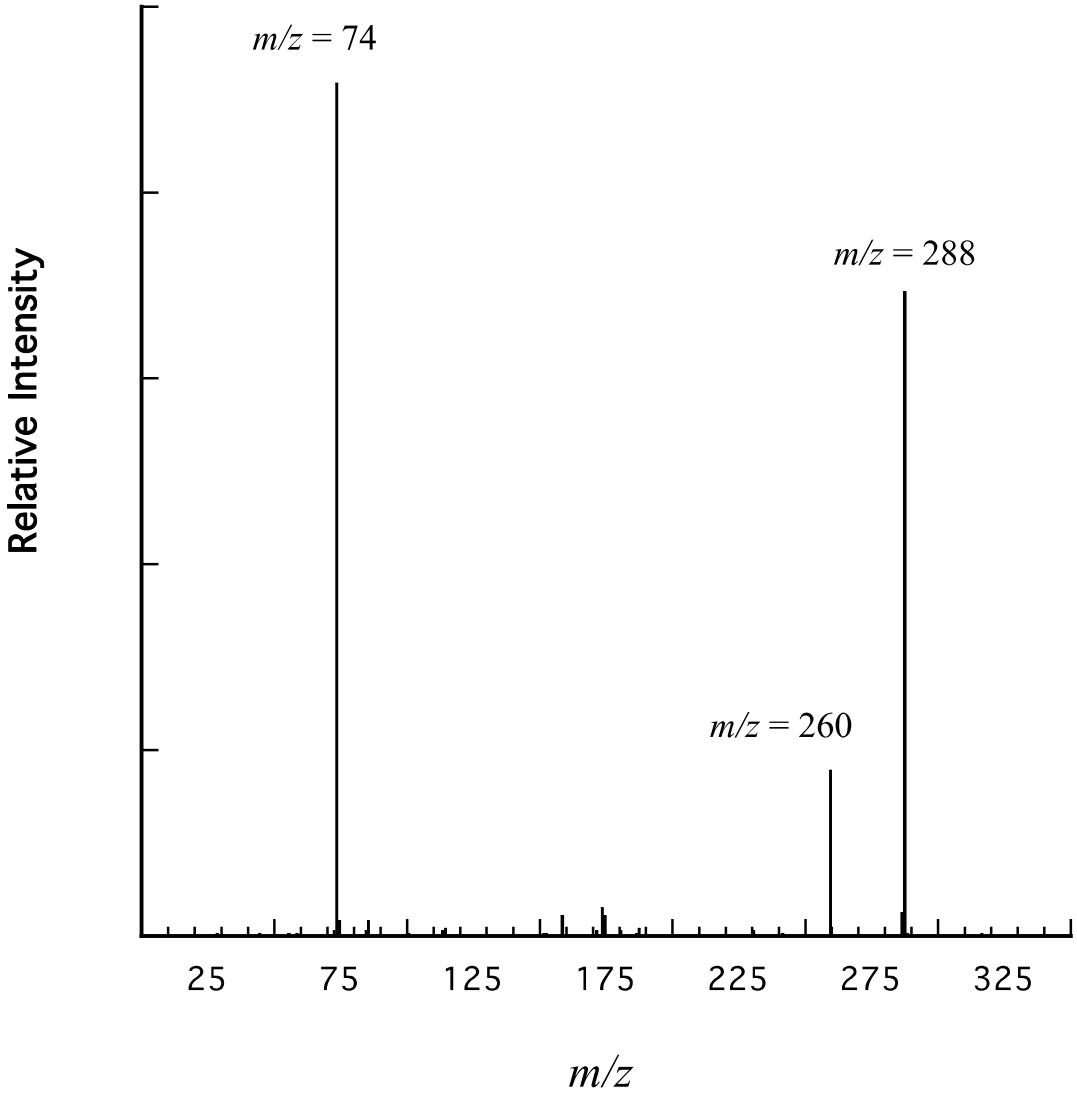
m/z = 74
m/z = 288
m/z = 260
Relative Intensity
25
75
125
175
225
275
325
m/z

Figure S4.

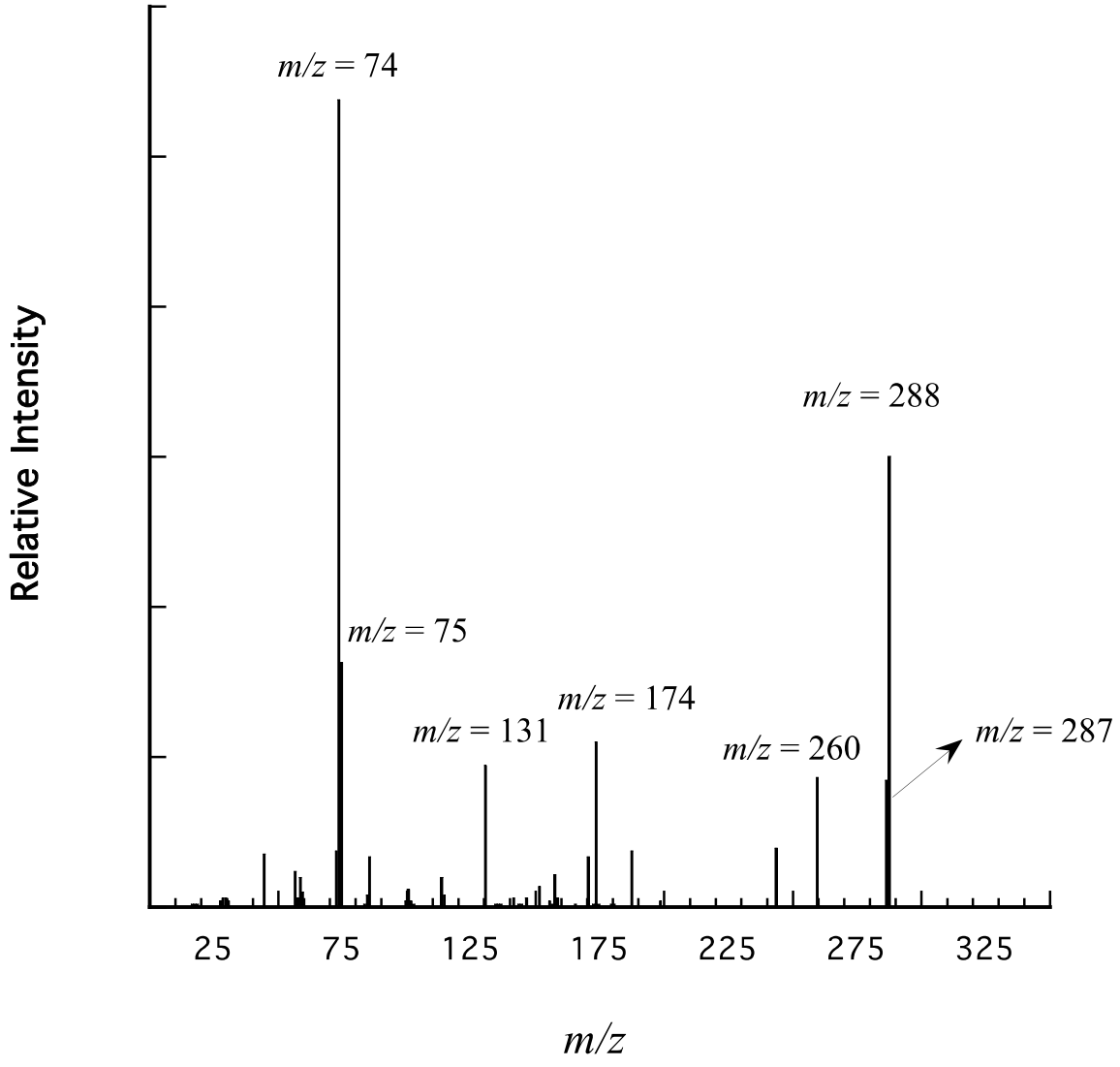
m/z = 74
m/z = 288
m/z = 75
m/z = 174
m/z = 131
m/z = 260
m/z = 287
Relative Intensity
25
75
125
175
225
275
325
m/z

Figure S5.

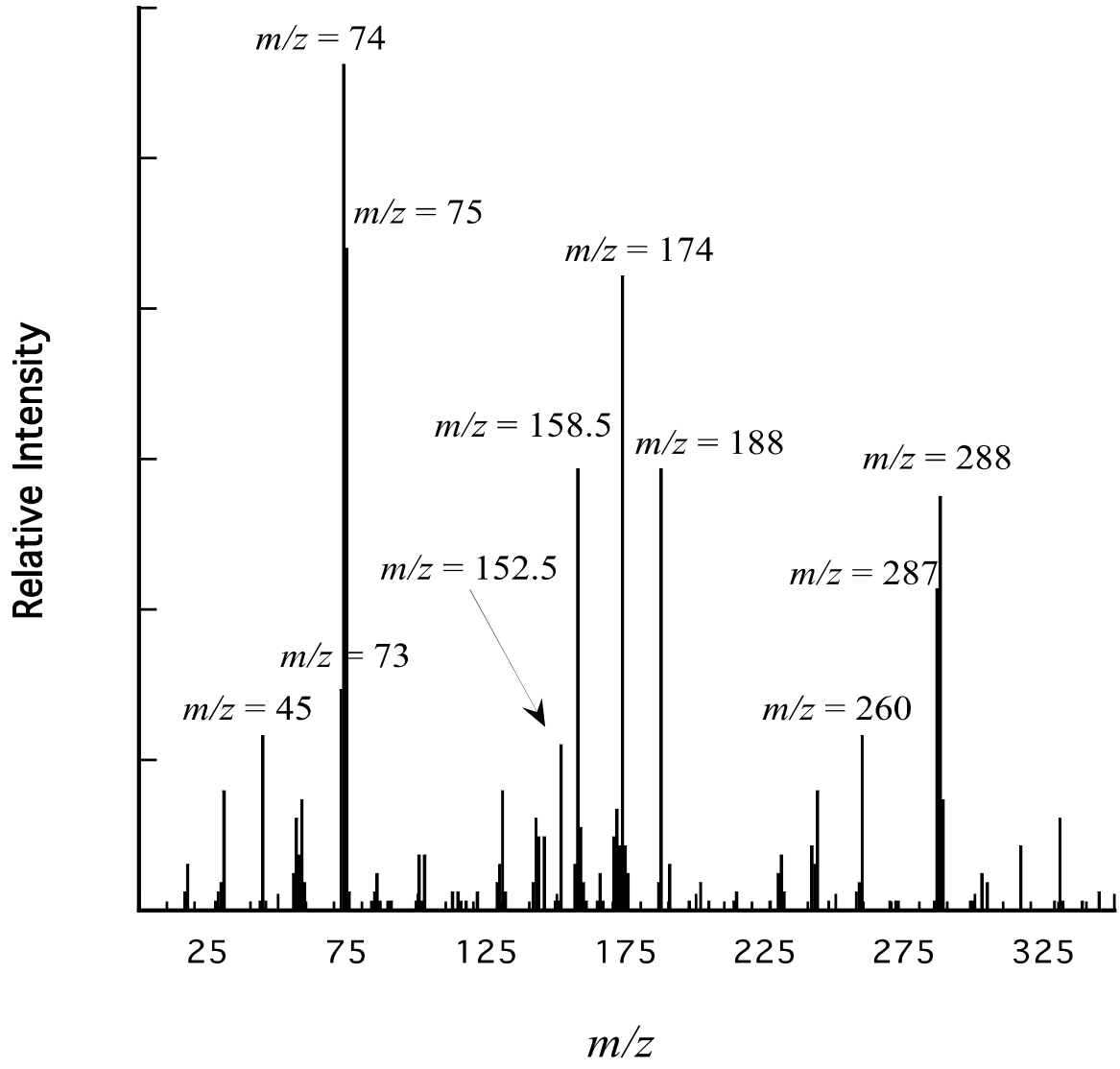
m/z = 74
m/z = 75
m/z = 174
m/z = 158.5
m/z = 188
m/z = 288
m/z = 152.5
m/z = 287
m/z = 73
m/z = 45
m/z = 260
Relative Intensity
25
75
125
175
225
275
325
m/z

Figure S6.

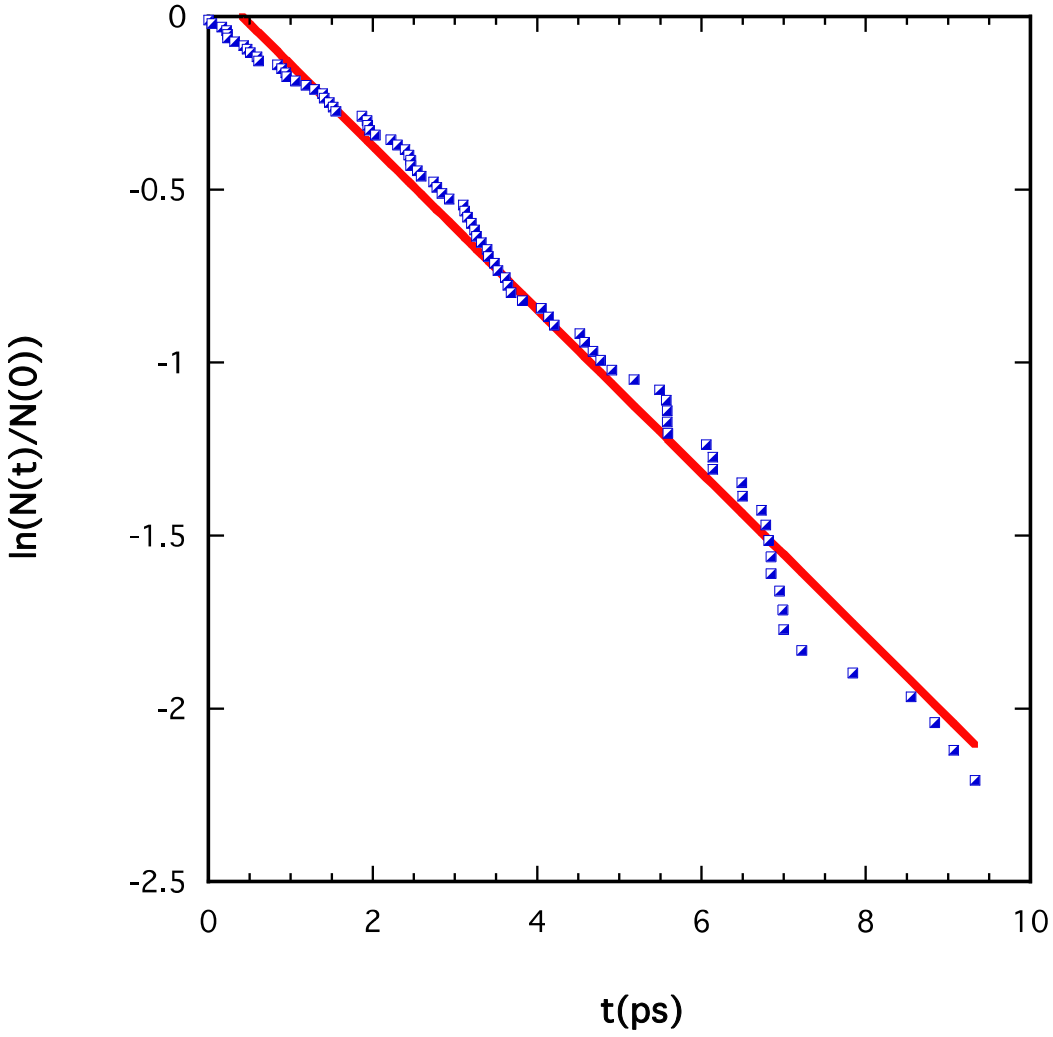

Figure S7.

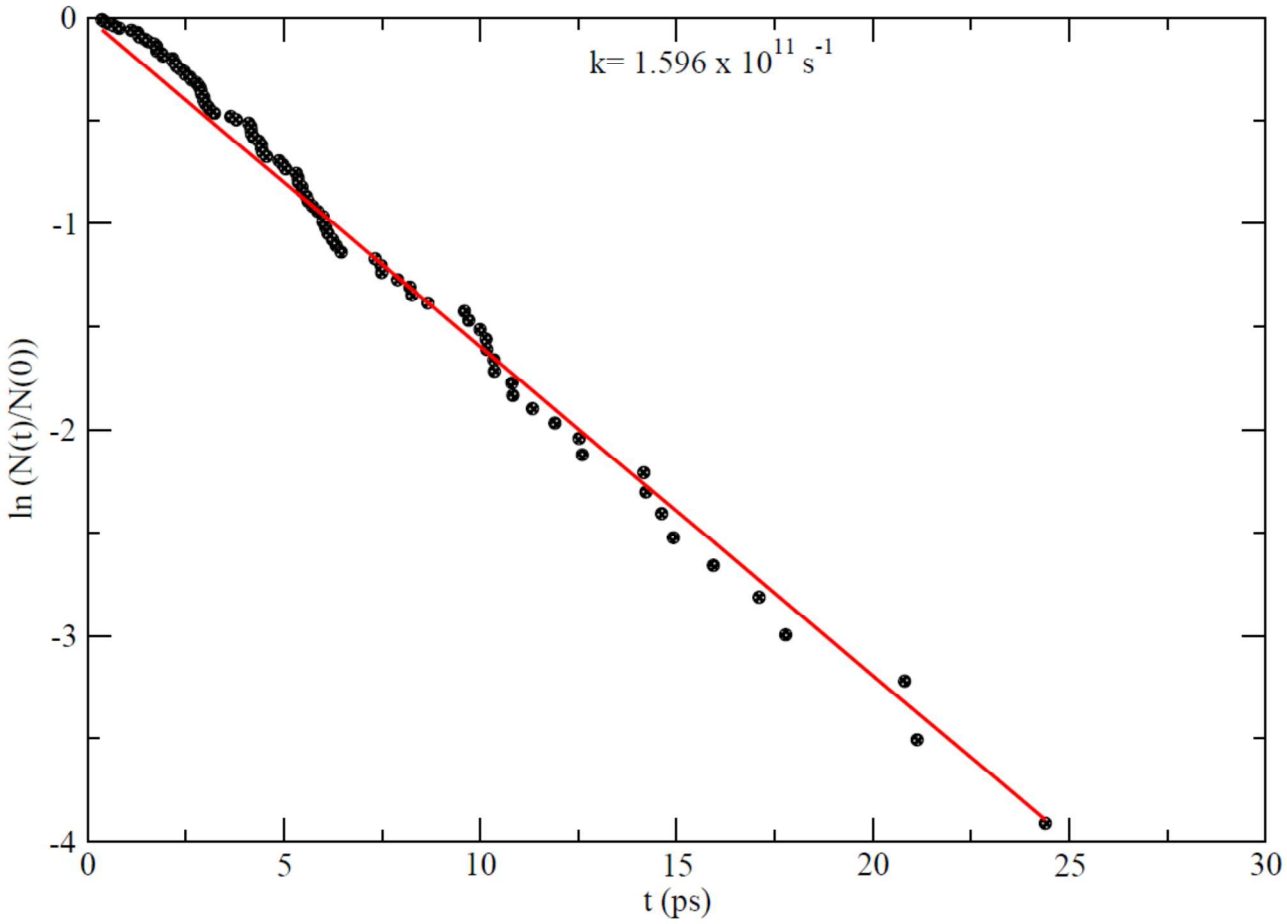

Figure S8

Secondary Dissociations from Path 1:

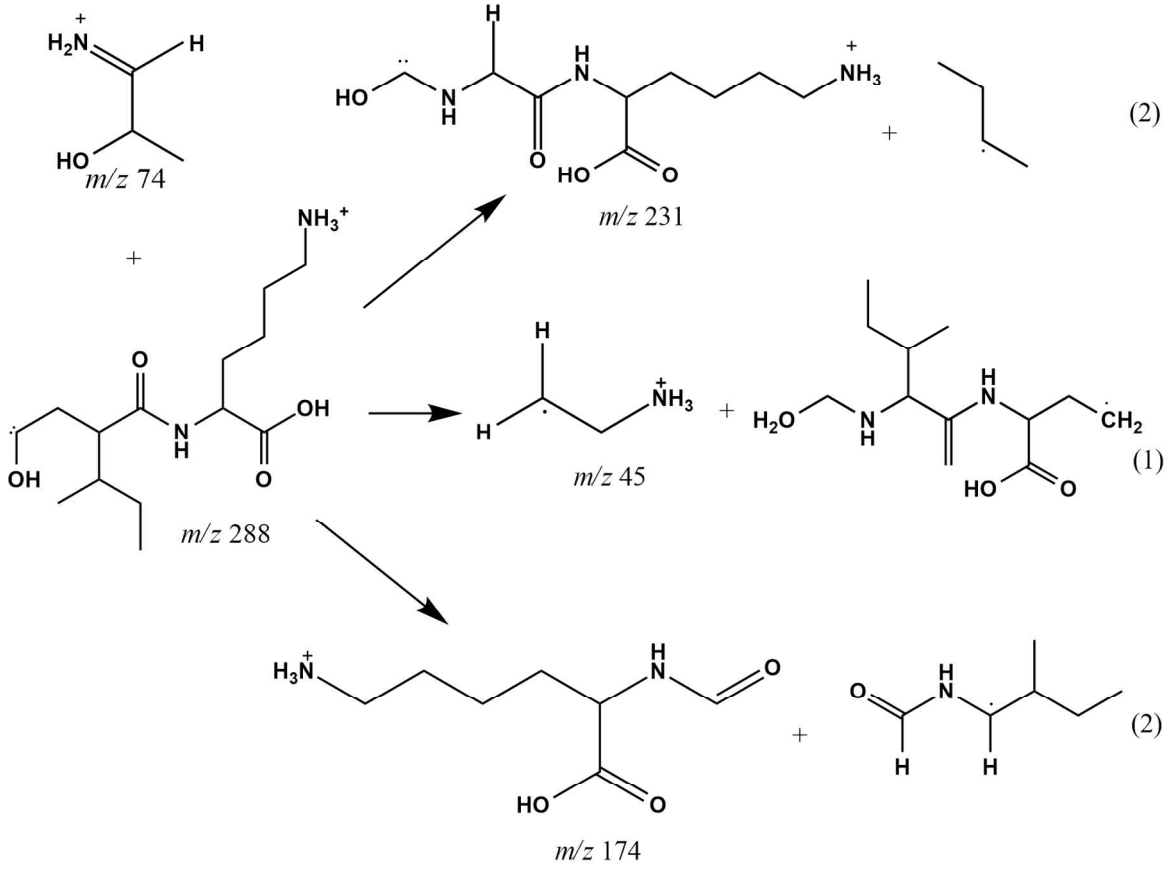

Secondary Dissociations from Path 3:

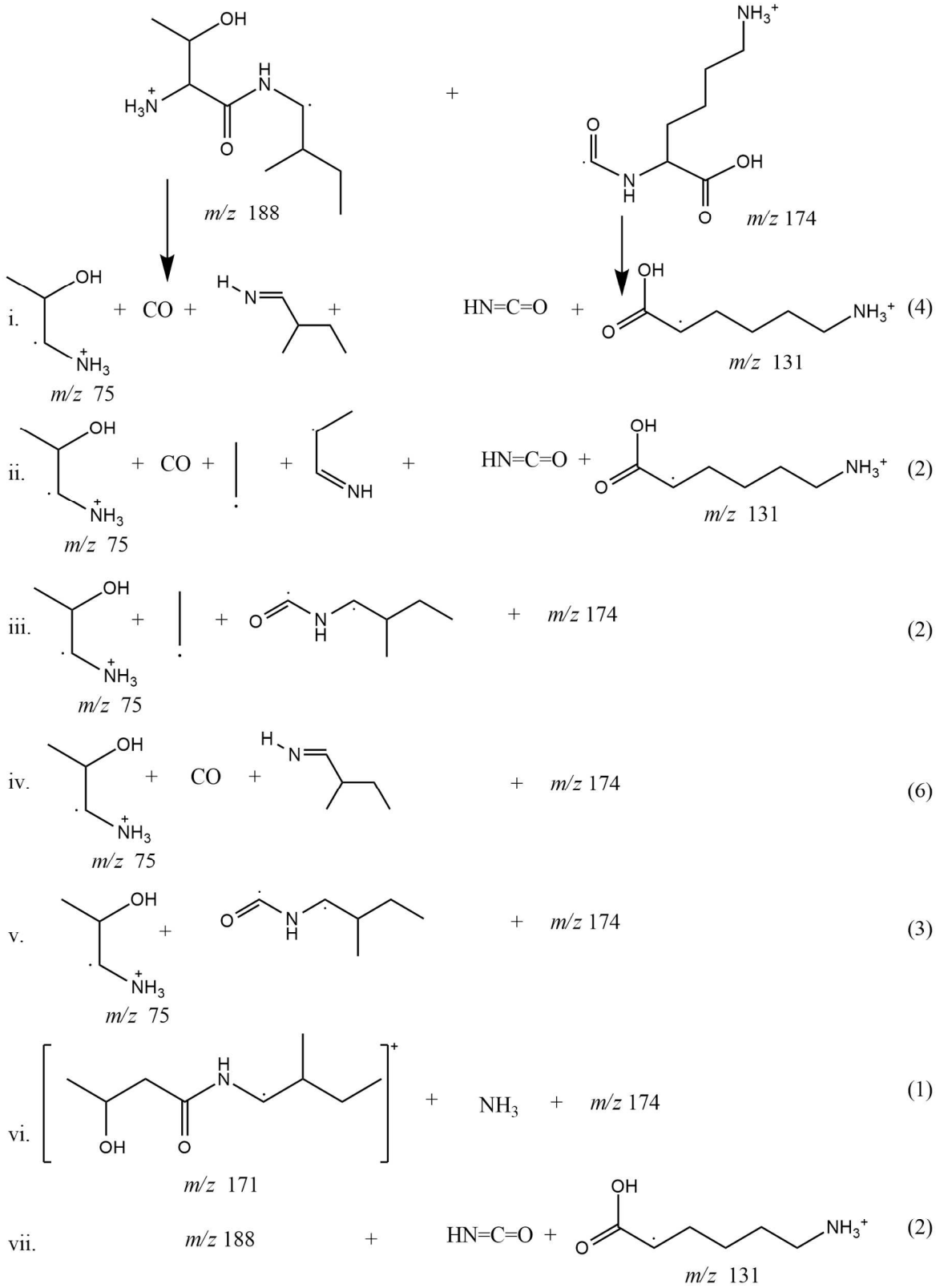

Secondary Dissociations from Path 4:

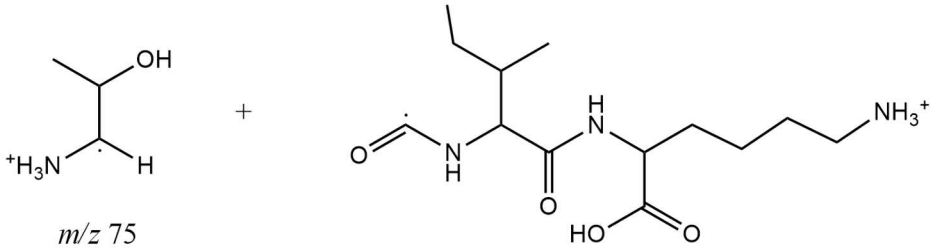

m/z 75

m/z 287

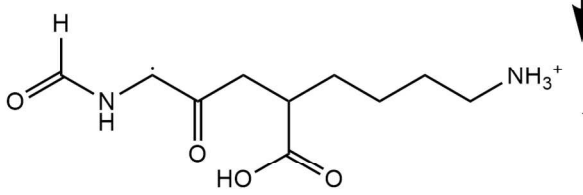

m/z 231

(2)

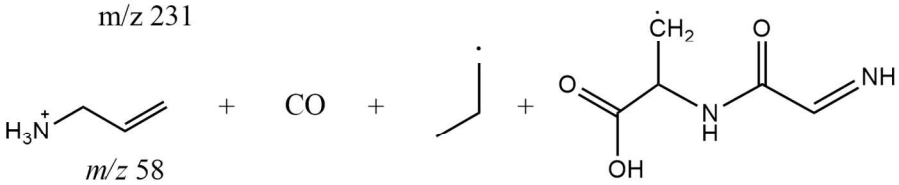

m/z 58

(3)

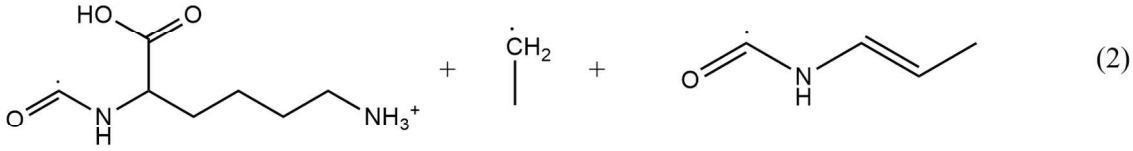

m/z 215

(2)

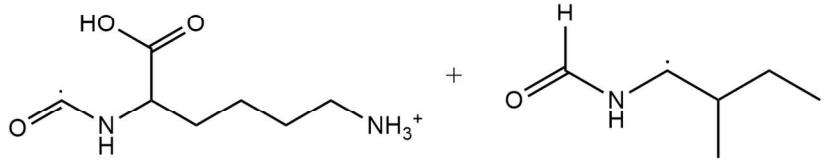

m/z 215

(3)

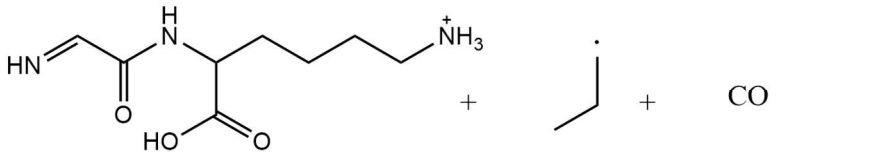

m/z 202

(3)

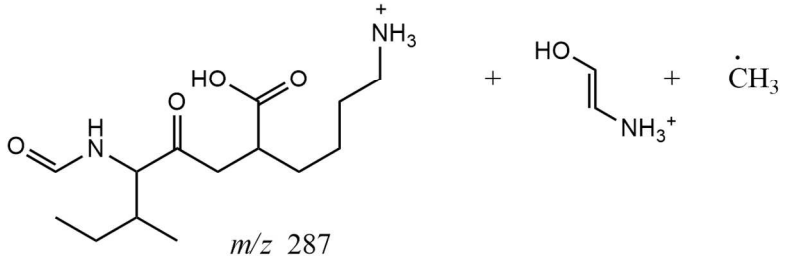

m/z 287

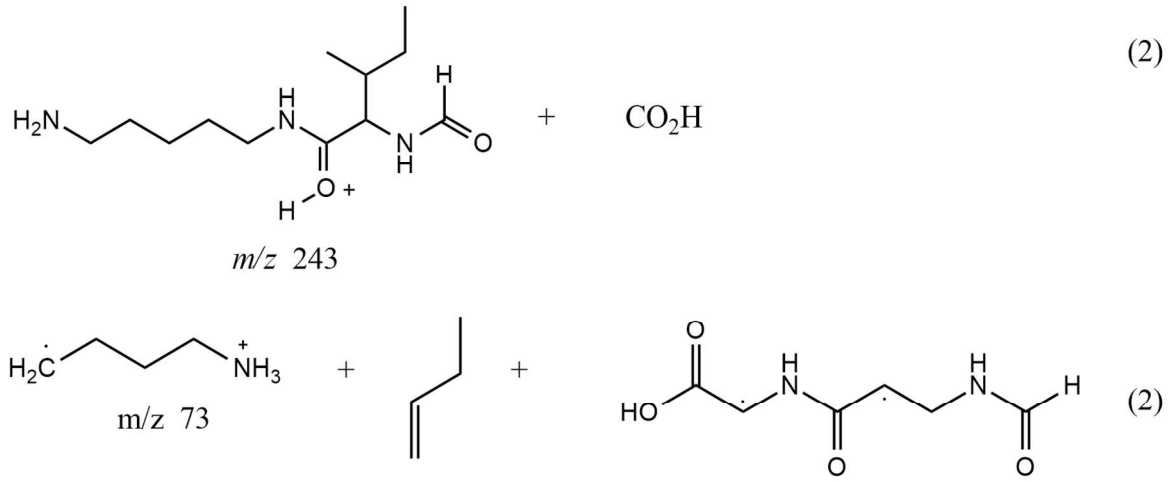

Secondary Dissociations from Path 6:

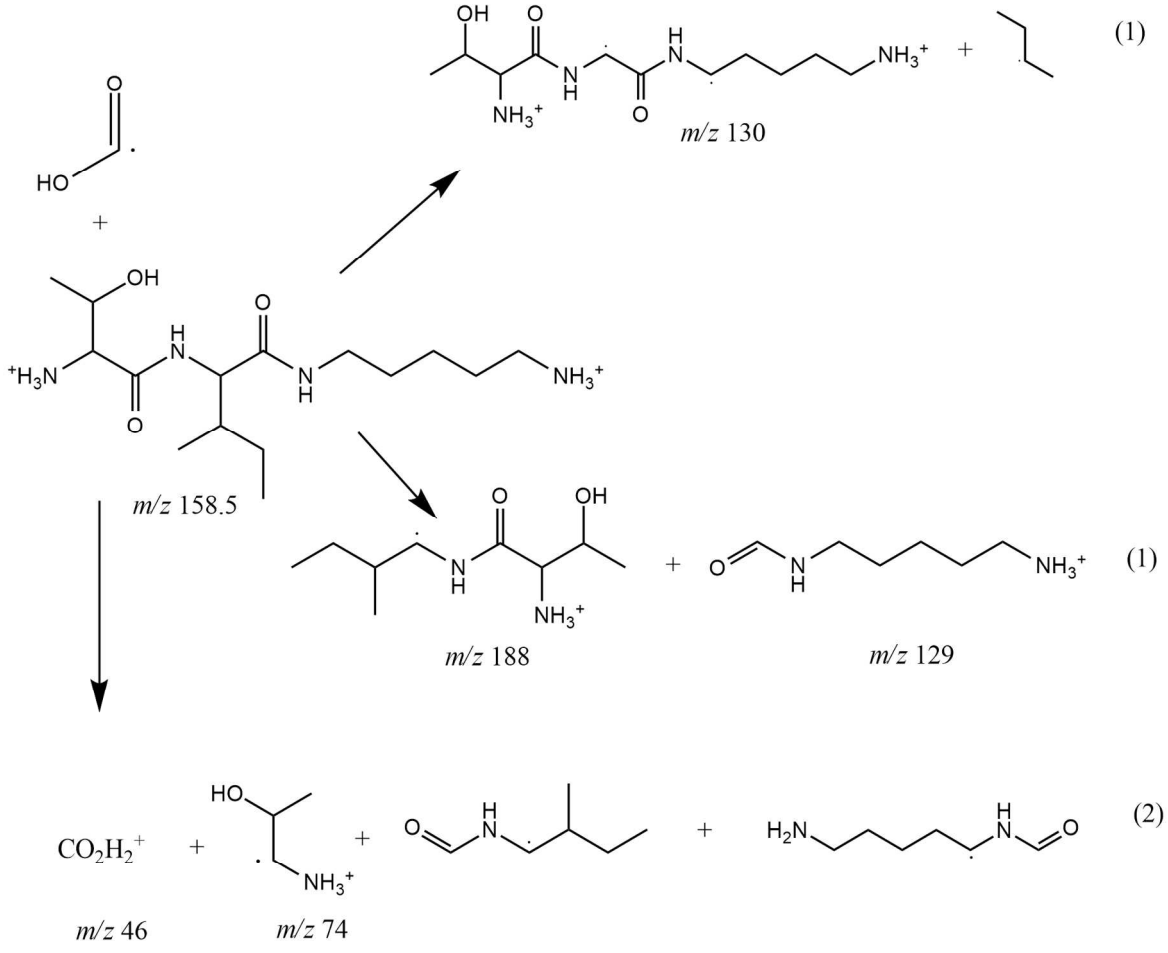

Secondary Dissociations from Path 7:

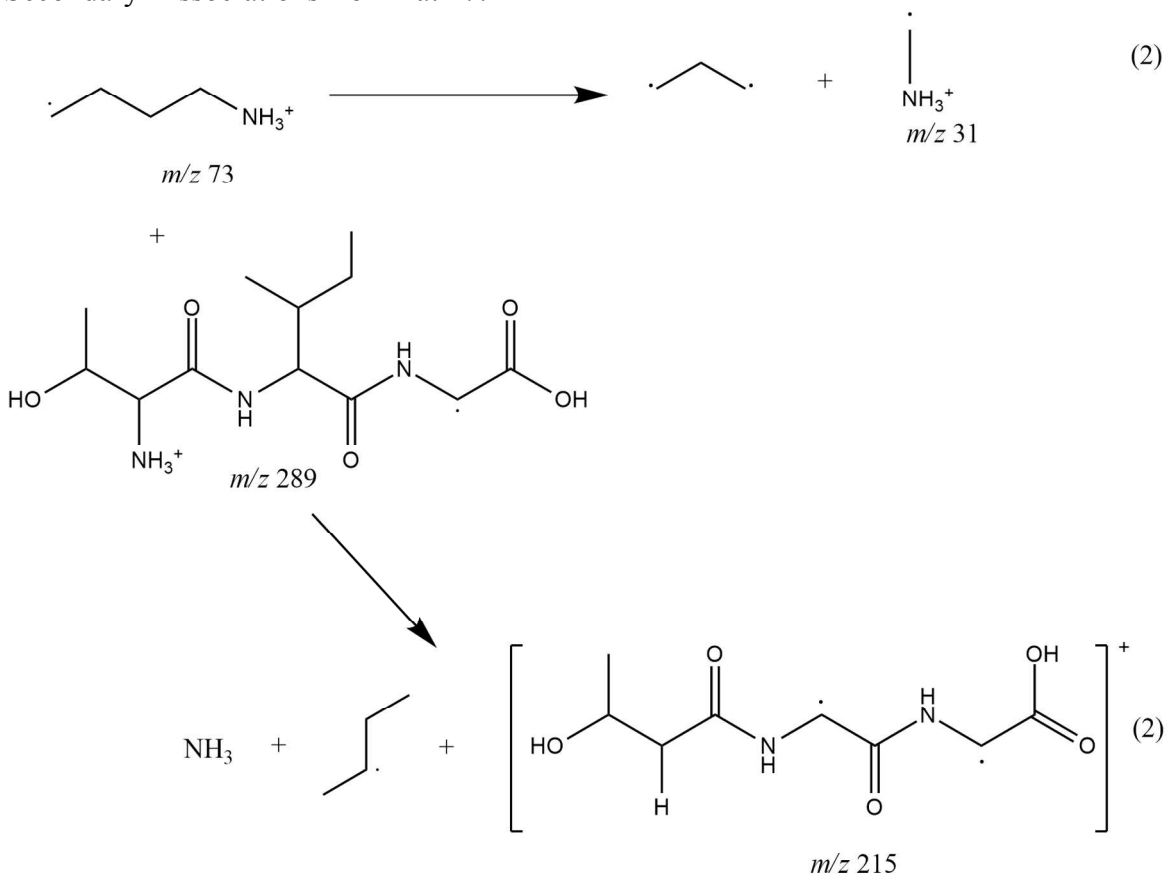

Secondary Dissociations from Path 8:

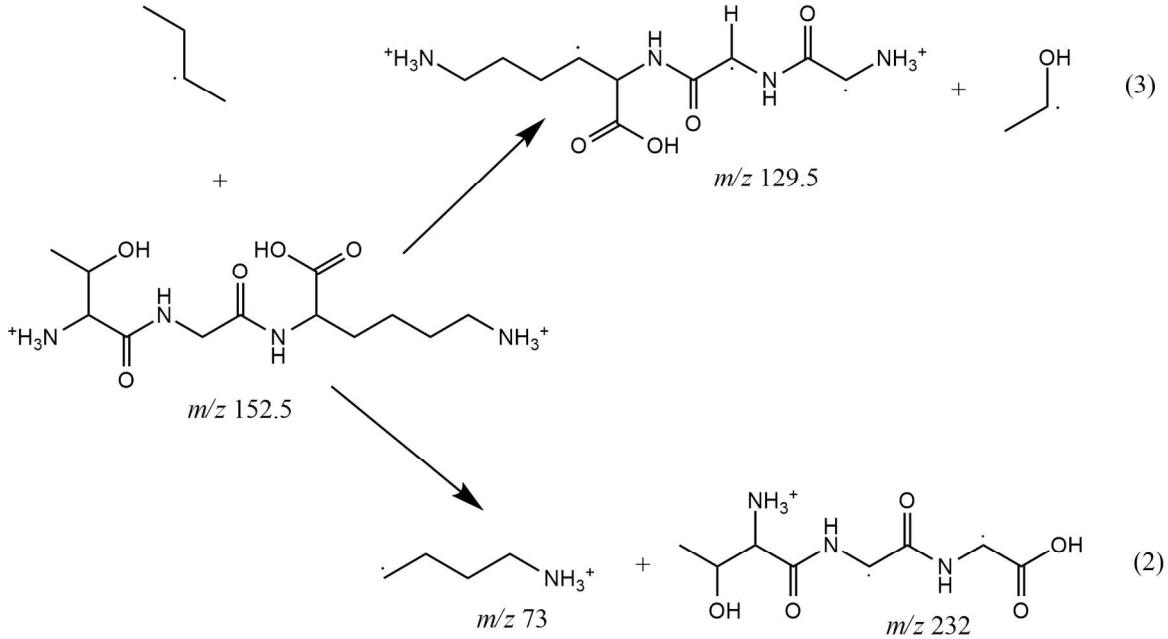

Secondary Dissociations from Path 9:

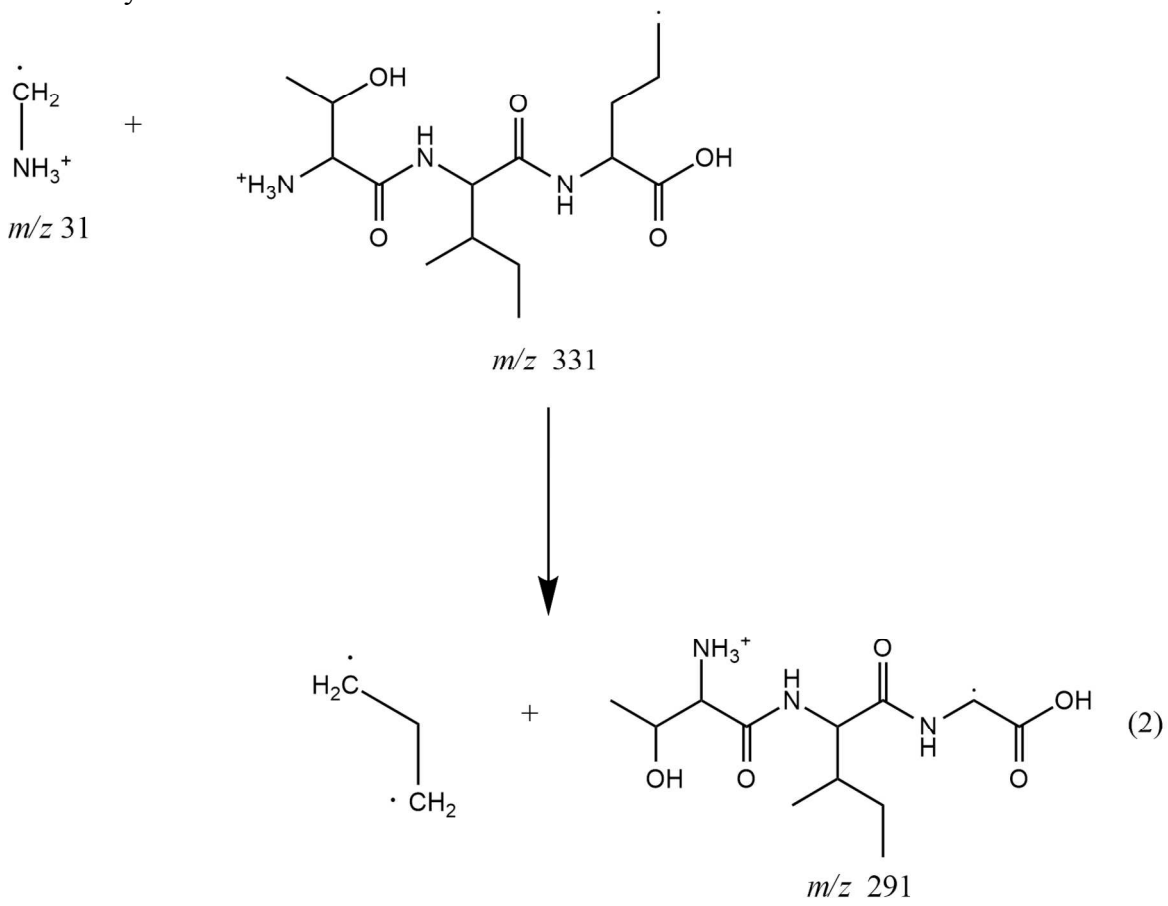

(2)

Secondary Dissociations from Path 13:

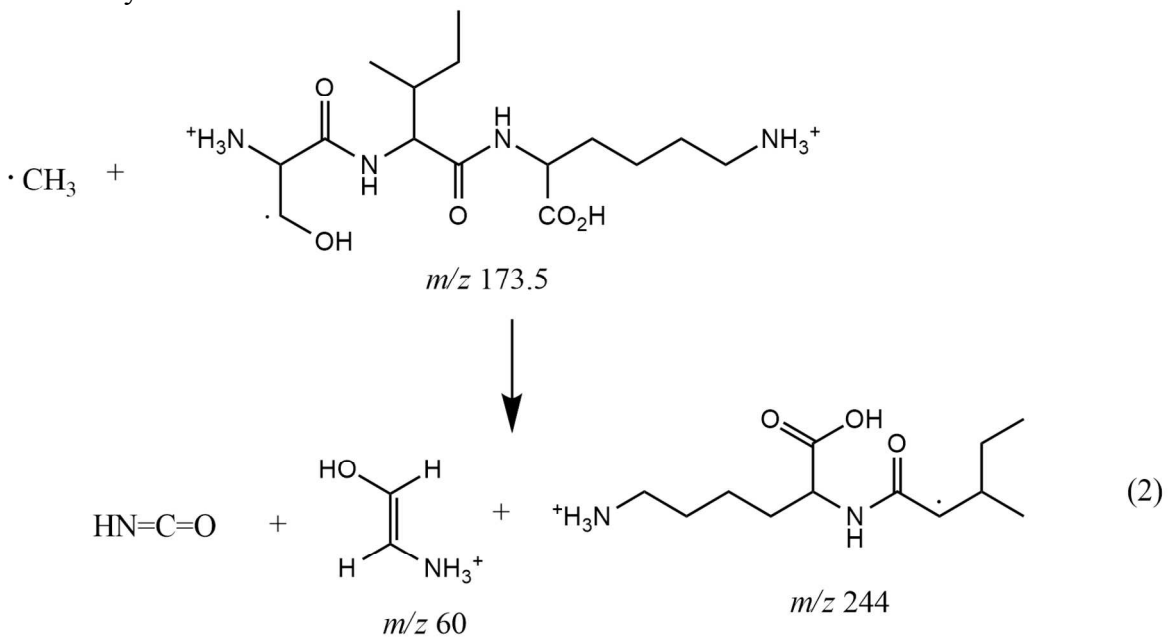

(2)

Secondary Dissociations from Path 15:

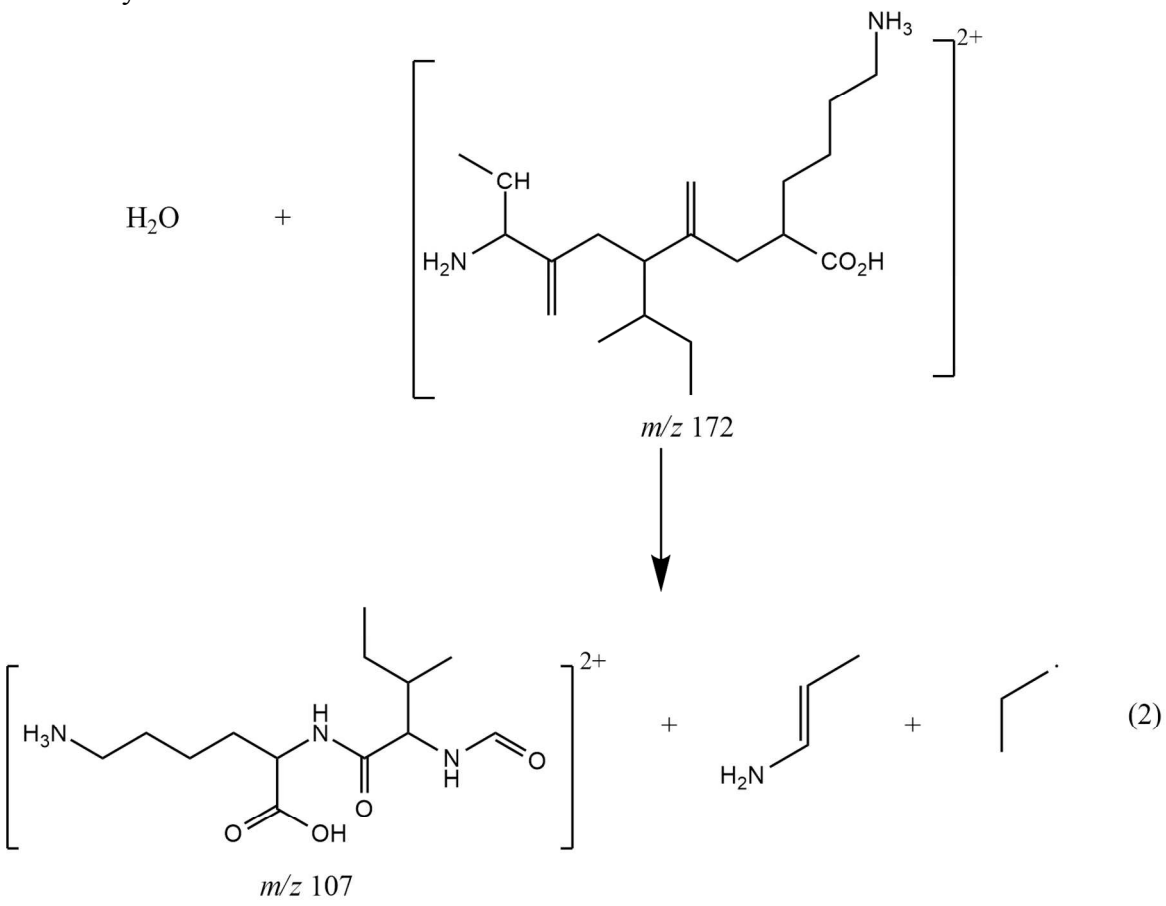

Secondary Dissociations from Path 17:

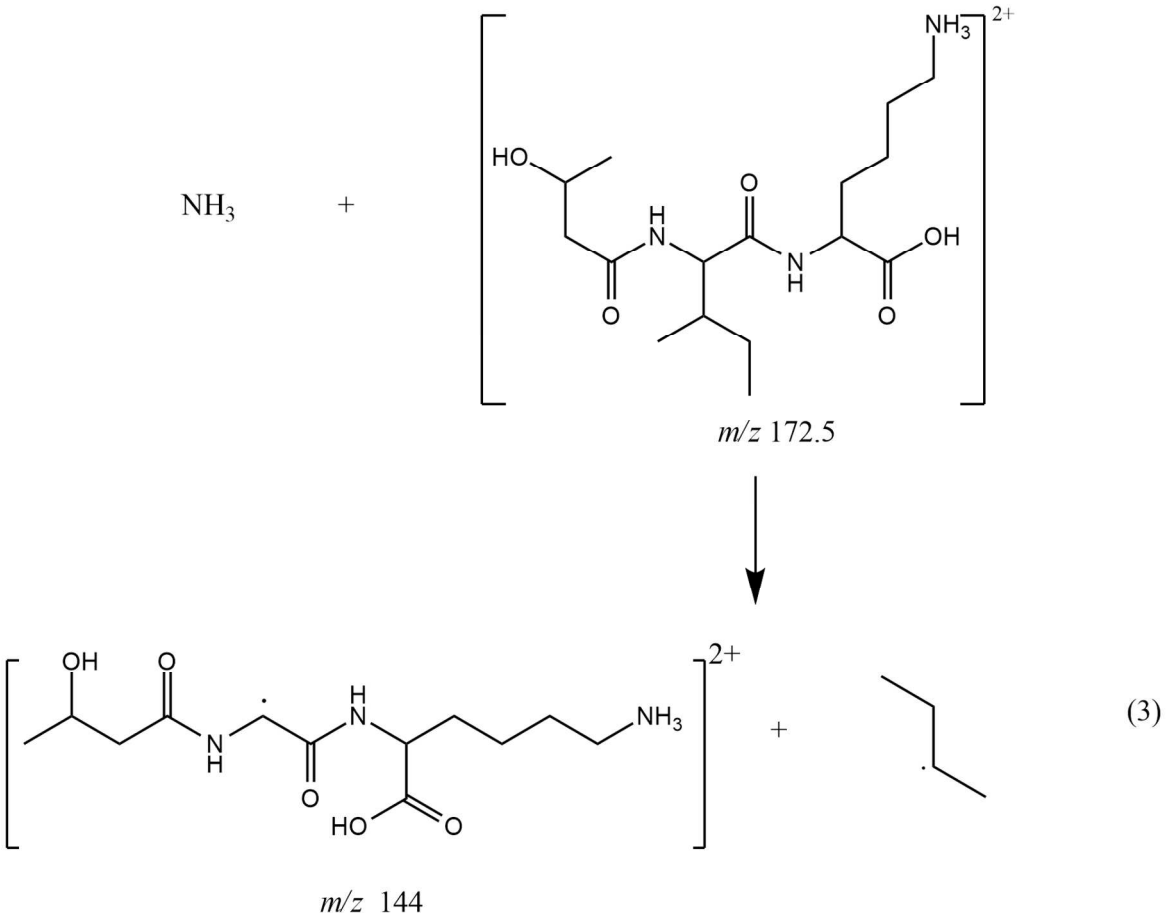

m/z 144

(3)

Secondary Dissociations from Path 18:

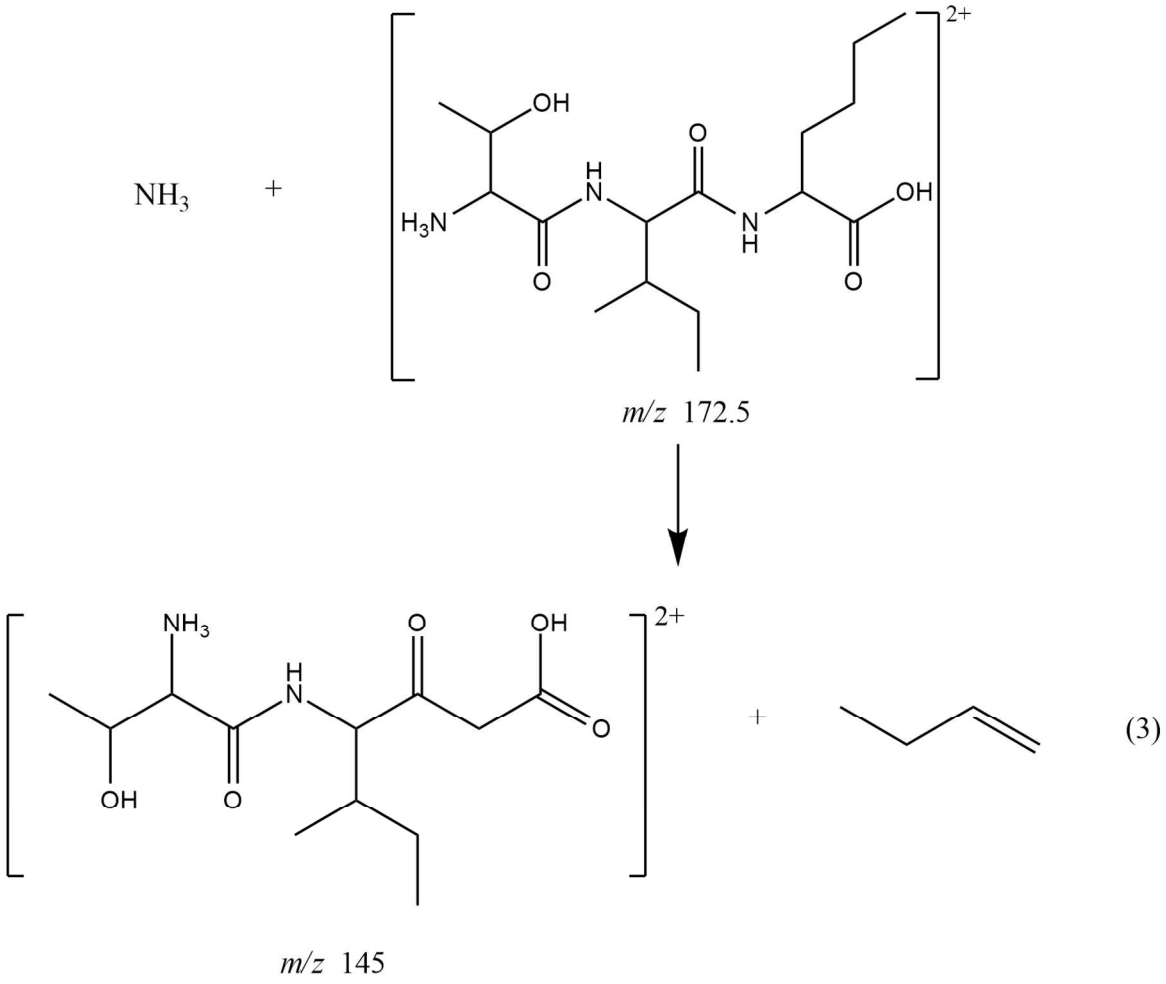

Figure S9.

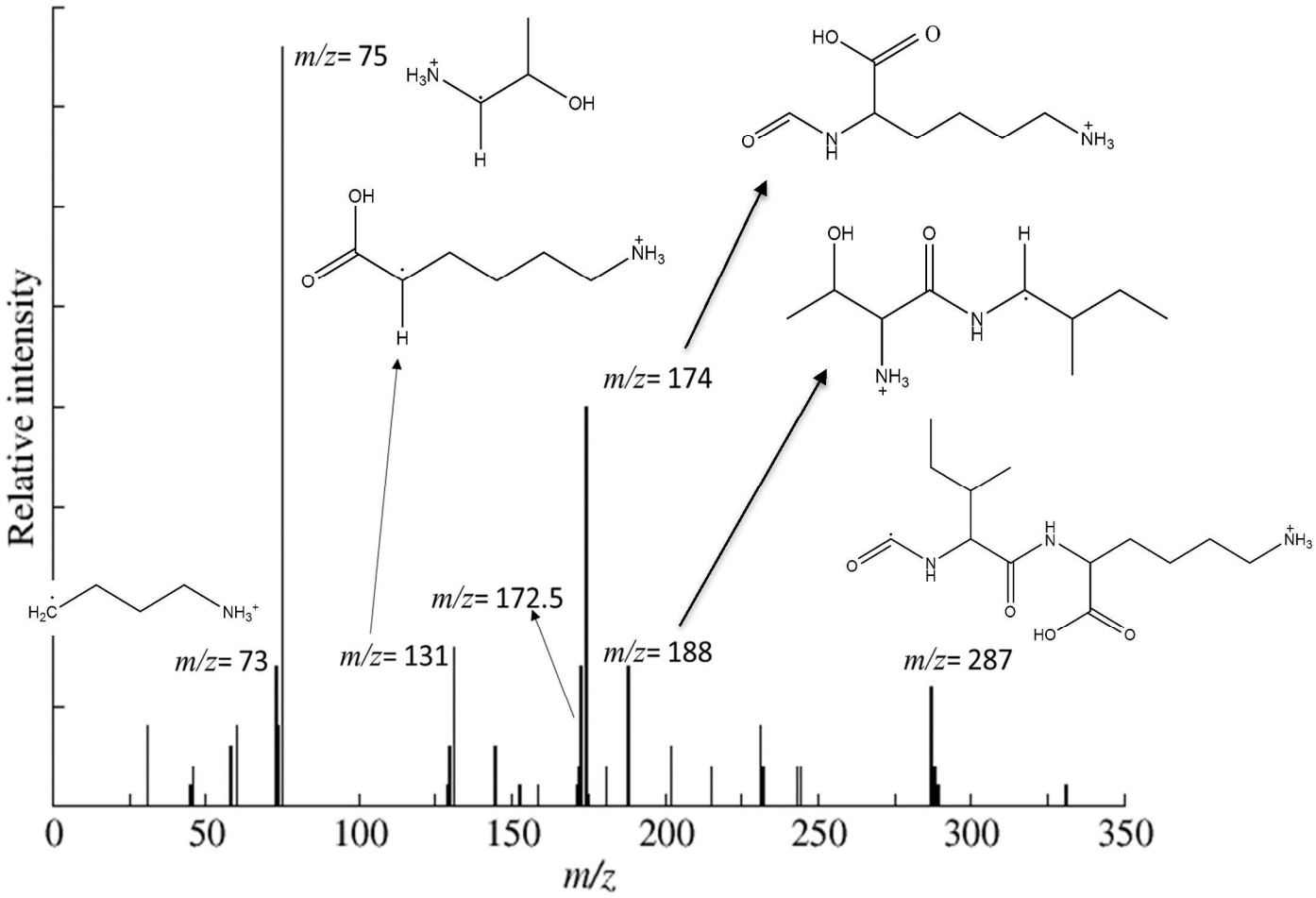
Relative intensity
m/z= 75
m/z= 73
m/z= 131
m/z= 172.5
m/z= 174
m/z= 188
m/z= 287
0
50
100
150
200
250
300
350
m/z

Figure S10.

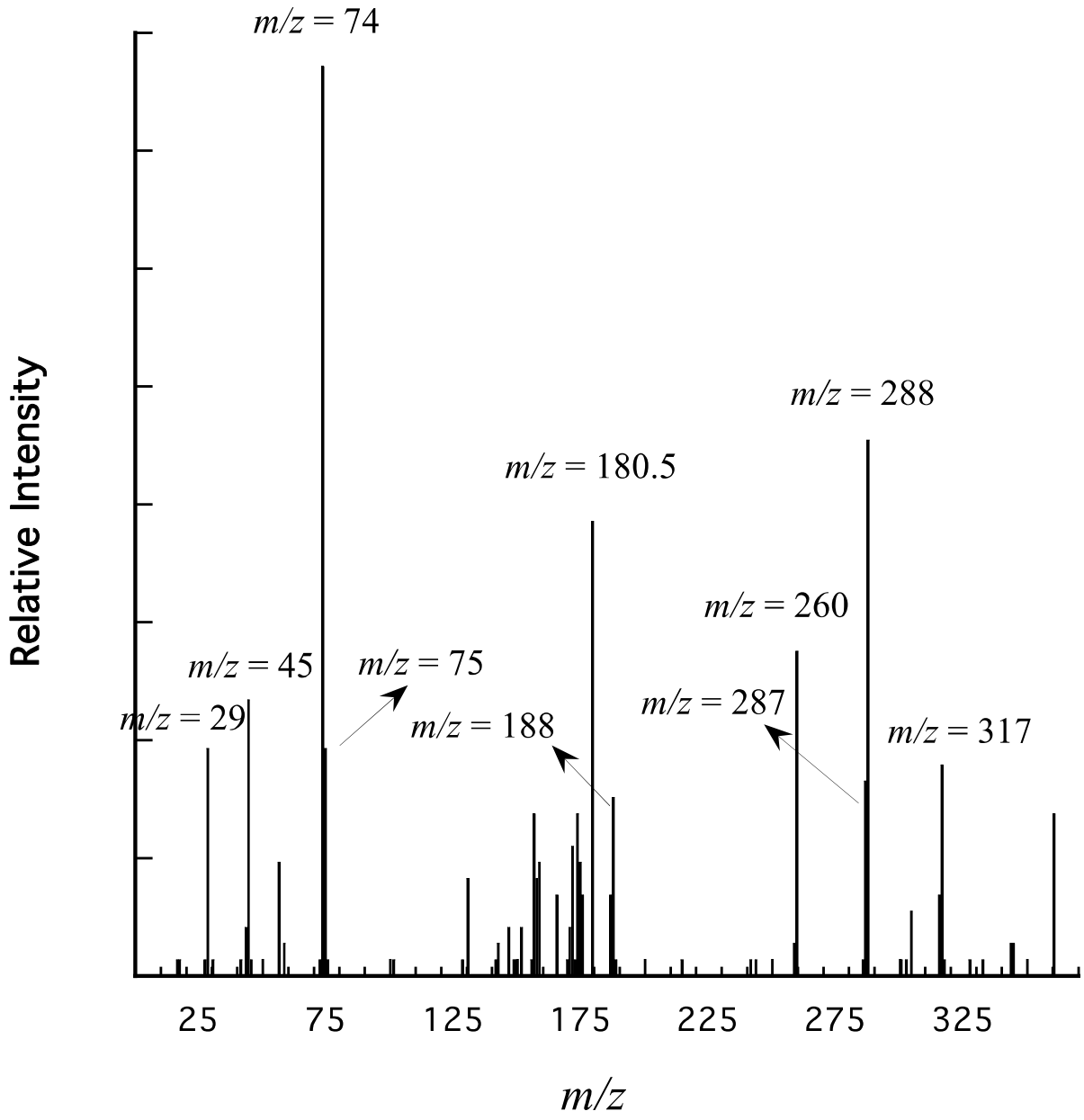
m/z = 74
m/z = 288
m/z = 180.5
m/z = 260
m/z = 45
m/z = 75
m/z = 29
m/z = 188
m/z = 287
m/z = 317
Relative Intensity
25
75
125
175
225
275
325
m/z

Figure S11.

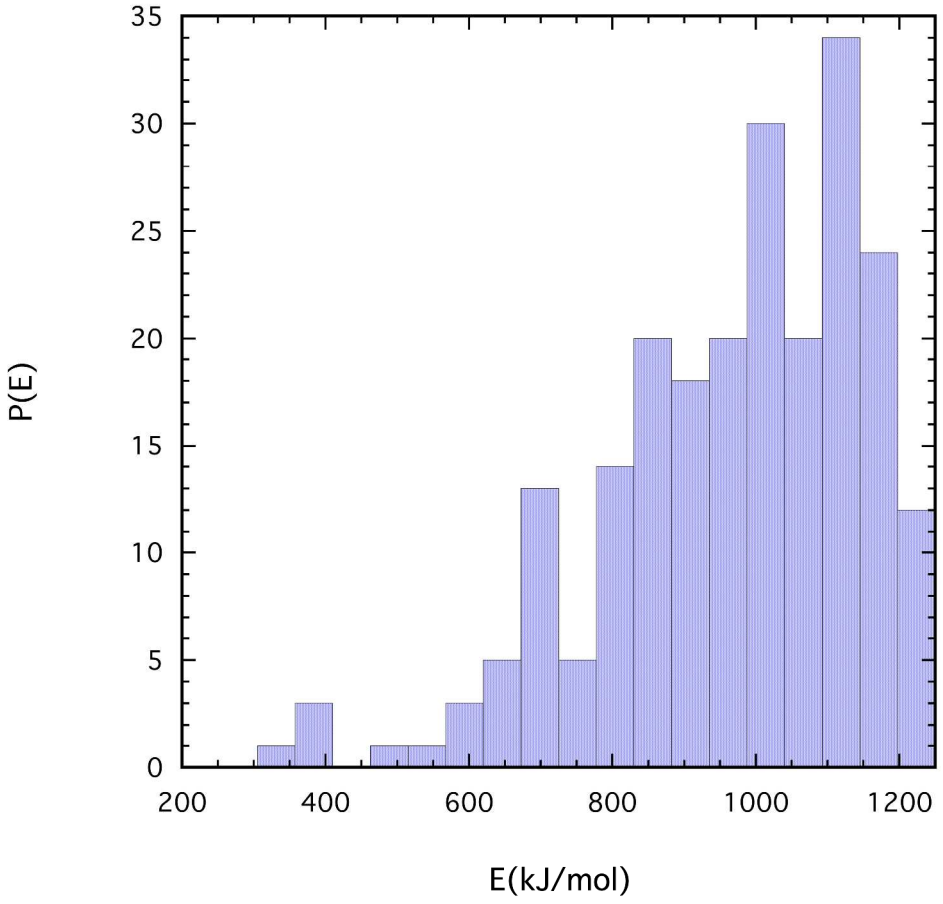

Figure S12.

Table S1. Probabilities of TIK$(H^+)_2$ Dissociation Pathways versus Temperature from RM1 Direct Dynamics Simulations for pathways 1-20.

	Temperature			
Pathway	1250	1500	2000	2500
1	85.5	73.2	35.4	12.9
2	12.1	18.7	9.6	4.5
3	2.4	0.8	12.6	16.5
4		1.6	15.2	10.9
5		1.1	6.7	8.1
6		0.3	2.2	3.6
7			1.7	2.4
8		0.5	3.9	1.6
9			0.8	2.4
10			0.4	1.6
11			0.2	1.2
12				0.4
13		0.3	1.1	1.2
14				0.4
15			0.4	1.6
16				0.8
17				0.4
18			0.8	1.2
19			0.4	0.4
20			0.9	0.8
Other paths		3.5	7.7	27.1

Table S2. Probabilities of different fragment ions (*m/z*) from RM1 calculations at 1250 K.

T = 1250 K	
m/z	Probability
74	48.7
288	42.5
260	6.0
188	1.2
174	1.2
114	0.2
242	0.2

Table S3. Probabilities of different fragment ions (*m/z*) from RM1 calculations at 1500 K.

T=1500K	
m/z	Probability
74	45.9
288	34.8
260	9
174	1.6
287	1.2
175	1.1
159	1.1
86	0.8
75	0.8
188	0.4
115	0.4
181	0.3
231	0.3
73	0.3
171	0.3
114	0.3
85	0.3
45	0.1
29	0.1
56	0.1
59	0.1
317	0.1
153	0.1
101	0.1
289	0.1
187	0.1
242	0.1
152.5	0.1

Table S4. Probabilities of different fragment ions (*m/z*) from RM1 calculations at 2000 K.

T = 2000 K			
m/z	Probability	*m/z*	Probability
74	26.9	272	0.3
288	15	147	0.3
75	8.1	30	0.3
174	5.5	142	0.3
131	4.6	28	0.2
260	4.3	259	0.2
287	4.2	245	0.2
244	2	100	0.2
73	1.8	31	0.2
188	1.8	199	0.2
45	1.8	102	0.2
86	1.7	156	0.2
171	1.7	158	0.1
243	1.3	144.5	0.1
57	1.2	181	0.1
317	1.2	166.5	0.1
158.5	1.1	180.5	0.1
59	1	136.5	0.1
114	1	173.5	0.1
146	0.8	17	0.1
143	0.8	18	0.1
152.5	0.7	19	0.1
175	0.7	173	0.1
101	0.6	157	0.1
215	0.6	103	0.1
231	0.6	218	0.1
60	0.5	144	0.1
242	0.5	225	0.1
289	0.4	271	0.1
202	0.4	136	0.1
85	0.4	135	0.1
203	0.4	258	0.1
115	0.4	230	0.1
58	0.3	84	0.1
29	0.3	345	0.1
159	0.3		

Table S5. Probabilities of different fragment ions (*m/z*) from RM1 calculations at 2500 K.

	T = 2500K				
m/z	Probability	*m/z*	Probability	*m/z*	Probability
74	11.2	243	0.6	142	0.2
75	8.8	18	0.6	248	0.1
174	8.4	130	0.6	160	0.1
188	5.9	191	0.6	166	0.1
158.5	5.9	56	0.6	28	0.1
288	5.5	173.5	0.6	167	0.1
287	4.3	175	0.6	115.5	0.1
73	2.9	180.5	0.5	198	0.1
45	2.3	166.5	0.5	151	0.1
260	2.3	230	0.5	205	0.1
152.5	2.2	86	0.5	214	0.1
31	1.6	303	0.5	227	0.1
131	1.6	60	0.4	329	0.1
244	1.6	259	0.4	330	0.1
289	1.5	30	0.4	44	0.1
59	1.5	305	0.4	114	0.1
172.5	1.4	158	0.4	46	0.1
57	1.3	187	0.4	102	0.1
143	1.3	202	0.4	332	0.1
331	1.3	129	0.4	270	0.1
159	1.1	85	0.2	300	0.1
144	1	143.5	0.2	299	0.1
171	1	76	0.2	286	0.1
146	1	130.5	0.2	273	0.1
242	0.9	113	0.2	272	0.1
317	0.9	17	0.2	84	0.1
172	0.9	29	0.2	118	0.1
173	0.9	232	0.2	87	0.1
103	0.8	345	0.2	90	0.1
101	0.8	115	0.2	91	0.1
58	0.8	258	0.2	100	0.1
231	0.7	215	0.2	150	0.1
157	0.6	122	0.2		

Table S6. Abundances of different fragment ions (*m/z*) from AM1 calculations when the trajectories were halted at 30 ps (2000K).

m/z	Abundance
75.07	38
174.2	20
287.	10
131.1	8
73.09	7
188.	7
174.	7
172.5	7
231.14	4
74.06	4
60.07	4
31.04	4
202.13	3
188.16	3
144.66	3
144.09	3
129.58	3
58.06	3
244.19	2
243.2	2
232.11	2
215.09	2
46.02	2
288	2
181	2
172	2
289.18	2
171.14	1
130.1	1
129.1	1
45.06	1
158.5	1
152.5	1
331	1

Table S7. Probabilities of different fragment ions (*m/z*) from RM1 calculations for CID at 1255 kJ/mol.

	CID		
m/z	Probability	*m/z*	Probability
74	15.4	143	0.6
288	9.1	259	0.6
180.5	7.7	59	0.6
260	5.5	344	0.6
45	4.7	333	0.3
29	3.8	31	0.3
75	3.8	328	0.3
317	3.5	18	0.3
287	3.3	28	0.3
188	3	149.5	0.3
361	2.7	17	0.3
173.5	2.7	102.5	0.3
158.5	2.7	171.5	0.3
172.5	2.2	42	0.3
57	1.9	286	0.3
159	1.8	318	0.3
174	1.8	46	0.3
158	1.7	73	0.3
131	1.6	301	0.3
316	1.4	102	0.3
166.5	1.4	129	0.3
187	1.3	142	0.3
175	1.3	156	0.3
305	1.1	173	0.3
172	0.8	303	0.3
44	0.8	189	0.3
147	0.8	215	0.3
152.5	0.8	242	0.3
180	0.6	244	0.3
345	0.6	76	0.3